Relativistic Valence Bond Theory and its application to metastable Xe_2.

S. Kotochigova[a], E. Tiesinga[a], and I. Tupitsyn[b]
[a] *National Institute of Standards and Technology, Gaithersburg, MD 20899, USA.*
[b] *Physics Department, St. Petersburg University, 198904 St. Petersburg, Russia.*

We present a new version of the relativistic configuration interaction valence bond (RCIVB) method. It is designed to perform an *ab initio* all-electron relativistic electronic structure calculation for diatomic molecules. A nonorthogonal basis set is constructed from numerical Dirac-Fock atomic orbitals as well as relativistic Sturmian functions. A symmetric reexpansion of atomic orbitals from one atomic center to another is introduced to simplify the calculation of many-center integrals. The electronic structure of the metastable ($5p^5 6s + 5p^5 6s$) Xenon molecule is calculated and the influence of different configurations on the formation of the molecule is analyzed.

I. INTRODUCTION

Recent years have seen a significant increase of interest in the *ab initio* valence bond (VB) approach [1,2]. Early interest in this method started with Heitler and London [3] who were the first to introduce the valence bond theory in the late twenties. The basic idea of the method is to construct the molecular wave function from atomic orbitals localized at the different atomic centers. Consequently the covalent bonding between atoms is described in terms of an "exchange effect" initiated by the overlap of orbitals of participating atoms. At large R the molecular wave function has a pure atomic form that appropriately describes the molecular dissociation limit. At short internuclear separations orbitals around different centers have considerable overlap or non-orthogonality which leads to a large exchange effect and creates a bond. Therefore it is crucial for the method to use a formalism incorporating the non-orthogonality of the basis wave functions. Application of the VB theory for many-electron molecules only became practical with the advent of large computers.

An important development for the valence bond theory was the use of "ionic structures", in which the participating atoms obtain positive and negative charges. Coulson and Fischer [4] showed that ionic structures included into the calculation lead to deformation of the atomic wave functions and hence to more realistic description of molecular formation.

Development of the VB theory was further directed towards optimization of the shapes of orbitals in order to introduce correlation effects. These models for electronic structure of a molecule were proposed by Goddard [5] and Gerratt [6]. The distinctive features of the model are that it takes into account the different ways of coupling the electron spins together to give total electron spin S and that the atomic orbitals are optimized by applying a direct minimization procedure. These ideas formed the basis of the spin-coupled theory [7] which was applied to the electronic structure of several diatomic molecules [8,9] whose spectroscopic constants showed a 90 - 95 % agreement with observed values. Its concepts have been used to develop sophisticated spin-coupled approaches [10,11,2,12–15] that take into account a considerable amount of the chemically significant electron correlation effects. Another development [5] lead to the so-called generalized valence bond method [16–18], which combines features of self-consistent field and spin-coupled approaches.

In a recent development of the method we incorporated numerical Hartree-Fock (HF) non-orthogonal atomic orbitals [19–22] to construct the molecular wave function. Unlike many applications of the VB theory where analytic atomic orbitals of Gaussian type are used as basis functions, this way of constructing molecular wave functions avoids the need for large basis sets. The analytic functions do not display a correct behavior at the nuclei and in the asymptotic region which thus require a large number of Gaussians. In our basis it seems sufficient to use a single HF orbital for each inner shell and a few additional excited orbitals to describe valence electrons. This is true because the atomic HF orbitals already form a good representation of the atom. They have the right number of nodes and are orthogonal with respect to other HF orbitals localized at the same center.

More crucial for the success of Refs. [19–22] is the implementation of a full configuration interaction (CI) procedure based on non-orthogonal basis functions. Each molecular configuration is constructed from atomic configurations, covalent or ionic. In turn each atomic configuration is described by Slater determinants constructed from the numerical HF orbitals.

In the current paper we introduce a relativistic development in valence bond theory. Much of the structure of Refs. [19–22] is retained in this relativistic version of VB theory with the primary difference being that the basis functions are now constructed from four-component atomic Dirac spinors. These functions are numerically obtained by solving the integro-differential Dirac-Fock (DF) equations for atoms. In addition to using DF functions to optimize our basis we use configurations with fractional occupation. These configurations are constructed using relativistic version of the Hyper-Hartree-Fock method [23]. In this approach every atomic configuration is described by a density matrix of mixed states corresponding to the configuration

average. In the relativistic calculations we average over all relativistic configurations which are created from the same non-relativistic configuration. This averaged configuration has the property that it is the solution of non-relativistic HF equations when the speed of light goes to infinity in the relativistic DF equations.

In a CI expansion, excited configurations help to describe the formation of the molecule. Describing these excited configurations on the basis of Dirac-Fock functions has proven to be ineffective because the DF orbitals increase rapidly in size with increasing general quantum number n. Moreover, a complete set of these functions contains, in addition to discrete functions, continuum functions which are clearly impractical computationally.

To improve the characteristics of the excited states we instead use a set of Sturmian functions. The idea to use Sturmian functions as virtual states to model correlation effects in an atom was first developed by Sherstuk and Pavinsky [24,25]. It was shown that these functions form a complete set of discrete functions with similar asymptotic behavior and orbital size as the occupied valence orbitals. These characteristics make Sturmian basis functions very efficient in describing correlation effects (See section II).

The one- and two-electron integrals are calculated using a modified Löwdin's reexpansion procedure [26]. The modification concerns the fact that Löwdin's method is not very efficient when reexpanding strongly localized orbitals. Instead the integration region is divided in two and in each region the slowly varying part of the basis function centered in the other region is reexpanded. This symmetric reexpansion has much faster convergence characteristics than the method proposed in Ref. [26].

Our approach is, in principle, an all-electron calculation, which, for instance, allows us to evaluate the electronic densities at the nuclear sites and to calculate hyperfine structure constants. Hence, the dynamics of all electrons in a molecule is accounted for. However, often this is not necessary. Deep lying orbitals do not take part in the molecular formation. Therefore we introduce core and valence orbitals, where core electrons will not participate in the CI.

The method is designed to calculate the electronic potential surfaces and other electronic properties of dimers composed of atoms with any nuclear charge Z, any number of electrons, and any level of excitation. In this report, it is applied here to obtaining the electronic potentials for two interacting Xe atoms. This method is very suitable for studying collisional problems, because it naturally provides the physically realistic description of interacting atoms at large internuclear separations.

There are two reasons for calculating the metastable Xe potentials. Firstly, it has been proposed that metastable noble gases such as xenon might be good candidates for Bose-Einstein Condensation [27]. Secondly, the analysis of recent experiment [28] which studied the real-time dynamics of ultra-cold collisions with metastable and double excited xenon atoms, requires a theoretical treatment of the potentials over a wide range of internuclear separations. This study is a first attempt to obtain *ab initio* relativistic electronic potentials of metastable Xe atoms. Previous semi-empirical investigation of metastable xenon gas has focused on the long-range interactions between two distant atoms [27]. However in many situations the intermediate and short internuclear separations are essential for a complete understanding of cold collisions. For instance, the ability to hold metastable atoms with a reasonable density in a magnetic or optical trap depends on the full shape of the adiabatic potential curves. The asymptotic description of the potential curves is not sufficient and an *ab initio* calculation is required. Notice that the ability to hold metastable Xe not only depends on the adiabatic potentials but also on the "width" of the potentials. This width describes Penning and associative ionization of colliding metastable Xe. This paper does not address these ionization issues.

II. ATOMIC BASIS FUNCTIONS FOR OCCUPIED AND UNOCCUPIED ORBITALS.

The numerical atomic Dirac-Fock wave functions that describe occupied molecular orbitals were obtained by solving integro-differential DF equations for the self-consistent field of the configuration average. The equations for the self-consistent field were derived by applying the Hartree-Fock method to the eigenvalue and eigenfunction problem of the relativistic energy operator

$$\hat{H} = \sum_i \hat{h}_i + \sum_{i \neq j} \hat{v}_{ij}, \tag{1}$$

for each atom, where $\hat{h}_i = c(\vec{\alpha}_i \vec{p}_i) + \beta_i c^2 - Z/r_i$ is the Dirac operator for an electron in the field of a nucleus of charge Z and $\hat{v}_{ij} = 1/|r_i - r_j|$ is the Coulomb operator for the electron-electron interaction; α and β are the Dirac matrices and c is the speed of light. We express all equations using atomic units where $\hbar = m_e = 1$. One atomic unit of length is 1 a.u. $= 0.0529177$ nm.

In the central-field approximation the single-particle wave function is a four-component Dirac spinor

$$\psi_{n\kappa\mu}(\vec{r}) = \frac{1}{r} \begin{pmatrix} P_{n\kappa}(r) & \chi_{\kappa\mu}(\theta,\vartheta) \\ iQ_{n\kappa}(r) & \chi_{-\kappa\mu}(\theta,\vartheta) \end{pmatrix}, \tag{2}$$

where $\vec{r}$ is the electron coordinate, $P_{n\kappa}(r)$ and $Q_{n\kappa}(r)$ are the large and small components of the wave function, respectively; $\chi_{\kappa\mu}(\theta,\vartheta)$ is the spin-orbit wave function, corresponding to an eigenvalue $\kappa = \ell(\ell+1) - (j+1/2)^2$, where ℓ and j are the orbital and total angular momentum quantum numbers and μ is the projection quantum number of j.

The antisymmetric N-electron atomic wave functions are obtained in Slater determinant form $det^A = det(\psi_1(\vec{r_1}), ..., \psi_N(\vec{r_N}))/\sqrt{N!}$ where the functions ψ_i are

of the form given in Eq. (2) and superscript A labels the atom. To construct a many-electron wave function which belongs to the configuration

$$K = (n_1 l_1 j_1)^{q_1} ... (n_A l_A j_A)^{q_A}$$

we select determinants in which q_1 one-electron functions belong to shell $n_1 l_1 j_1$, and so on. Notice that for convenience we use the notation $n\ell j$ instead of $n\kappa$ to label the orbital $\psi_{n\kappa\mu}$. Both notations uniquely define a relativistic orbital. Note also that every non-relativistic configuration has split into several relativistic configurations.

Atomic configurations with fractional occupation are constructed for the orbitals in open shells. Fractional occupation is introduced via a configuration average. The average of Dirac-Fock orbitals is taken over all states of each relativistic configuration and all relativistic configurations belonging to the same non-relativistic configuration. This averaging ensures convergence of Dirac-Fock solutions to the non-relativistic Hartree-Fock solutions when the speed of light is infinity.

The unoccupied or virtual orbitals are described by Sturmian functions. These Sturmian orbitals are obtained by solving integro-differential Dirac-Fock-Sturm equations. These equations can be derived from the DF equations for occupied valence orbitals. The Coulomb interaction between electron and nucleus in these equations is multiplied with a factor λ. Furthermore, the one-electron energy is held constant at the energy of a valence electron. Solving these equations for eigenvalues $\lambda > 1$ we obtain a complete set of eigenfunctions. The complete set of these Sturmian functions is discrete and each orbital has approximately the same radius and the same asymptotic behavior as the corresponding valence orbital. These Sturmian orbitals help to construct excited configurations and lead to a compact and rapidly converging CI procedure.

III. MOLECULAR WAVE FUNCTION

The total molecular wave function Ψ_{AB} for a N-electron two-atomic molecule AB is introduced as a linear combination of molecular Slater determinants det_α^{AB},

$$\Psi_{AB} = \sum_\alpha C_\alpha det_\alpha^{AB} \tag{3}$$

where every molecular determinant is the antisymmetrized product of two atomic determinants

$$det_\alpha^{AB} = \hat{A}(det_\alpha^A \cdot det_\alpha^B) \tag{4}$$

The coefficients C_α in (3) are obtained by solving a generalized eigenvalue matrix problem described by the equation

$$\hat{H}_{AB}\vec{C} = E\hat{S}_{AB}\vec{C}, \tag{5}$$

where $\hat{H}_{AB}$ is the Hamiltonian matrix of atoms A and B and their mutual Coulomb interactions. The nonorthogonality matrix $\hat{S}_{AB}$, which is a scalar product of Slater determinants, is given by

$$(\hat{S}_{AB})_{\alpha\beta} = < det_\alpha^{AB} \mid det_\beta^{AB} > = (D_{\alpha\alpha}D_{\beta\beta})^{-1/2} D_{\alpha\beta}, \tag{6}$$

where $D_{\alpha\beta} = det| < \alpha_i|\beta_j > |$ is the determinant of the matrix of overlap integrals
$S_{i,j}^{\alpha\beta} = < \alpha_i|\beta_j >$ between orbitals α_i and β_j belonging to Slater determinants det_α^{AB} and det_β^{AB}, respectively. The α_i (β_j) stand for atomic orbitals $\psi_{n\kappa}(\vec{r})$ centered at either nucleus A or B.

It is convenient to define one- and two-particle density transition matrices. The one-particle density matrix is given by

$$\rho_1^{\alpha,\beta}(\vec{r},\vec{r}\,') = (D_{\alpha\alpha}D_{\beta\beta})^{-1/2} \cdot D_{\alpha\beta} \times \sum_{i,j}^{N} (S^{-1})_{i,j}^{\alpha,\beta} \cdot \psi_i(\vec{r}) \cdot \psi_j^*(\vec{r}\,'), \tag{7}$$

where $\psi_i(\vec{r})$ and $\psi_j^*(\vec{r}\,')$ are atomic orbitals and the two-particle density matrix is

$$\rho_2^{\alpha,\beta}(\vec{r_1},\vec{r_2}|\vec{r_1}\,',\vec{r_2}\,') = (D_{\alpha\alpha}D_{\beta\beta})^{-1/2} \sum_{i\neq k}^{N}\sum_{j\neq l}^{N} D_{i,j,k,l}^{\alpha,\beta} \times \psi_i(\vec{r_1}) \cdot \psi_j^*(\vec{r_1}\,') \cdot \psi_k(\vec{r_2}) \cdot \psi_l^*(\vec{r_2}\,'), \tag{8}$$

where

$$D_{i,j,k,l}^{\alpha\beta} = D_{\alpha\beta} \cdot \varepsilon_{i,k} \cdot \varepsilon_{j,l} \cdot [(S^{-1})_{i,j}^{\alpha,\beta} \cdot (S^{-1})_{k,l}^{\alpha,\beta} - (S^{-1})_{i,l}^{\alpha,\beta} \cdot (S^{-1})_{k,j}^{\alpha,\beta}]$$

$$\varepsilon_{i,k} = \begin{cases} 1 & i < k \\ -1 & i > k \end{cases} . \tag{9}$$

Introducing the Hamiltonian $\hat{H}_{AB}$ through one- and two-electron terms and the Coulomb repulsion u_{AB} between the nuclei,

$$\hat{H}_{AB} = \sum_{i=1}^{N} \hat{h}_i + \sum_{i\neq j}^{N} \hat{v}_{ij} + u_{AB}\,, \tag{10}$$

we describe one-electron matrix elements using Eq. (7) in the form [1]

$$< det_\alpha^{AB}| \sum_{i=1}^{N} \hat{h}_i |det_\beta^{AB} > = (D_{\alpha\alpha}D_{\beta\beta})^{-1/2} \cdot D_{\alpha\beta} \times \sum_{i,j=1}^{N} (S^{-1})_{i,j}^{\alpha,\beta} \cdot < \alpha_i|\hat{h}|\beta_j >, \tag{11}$$

where

$$\hat{h} = c(\vec{\alpha}\vec{p}) + \beta c^2 - \frac{Z_A}{|\vec{r} - \vec{R}_A|} - \frac{Z_B}{|\vec{r} - \vec{R}_B|}, \qquad (12)$$

and where R_A, and R_B are the nuclear coordinates. See Section IV for more details.

Two-electron matrix elements are obtained using Eq. (8) in the form [1]

$$< det_\alpha^{AB} | \sum_{i \neq j}^{N} \hat{v}_{ij} | det_\beta^{AB} >= (D_{\alpha\alpha} D_{\beta\beta})^{-1/2} \sum_{i,k=1}^{N} \sum_{j,l=1}^{N} \times D_{i,j,k,l}^{\alpha\beta} < \alpha_i, \alpha_j | \frac{1}{r_{12}} | \beta_k, \beta_l >, \quad (13)$$

where the evaluation of the two-electron matrix element $< \alpha_i, \alpha_j | 1/r_{12} | \beta_k, \beta_l >$ will be discussed in Sections V and VI.

IV. WAVE FUNCTION REEXPANSION

Two-center integrals are calculated using a symmetrical reexpansion procedure when a product of two wave functions localized at different centers appears in the integrands. The reexpansion procedure is based on techniques proposed by Löwdin [26]. Assume that the atomic nuclei are situated at position A and B respectively (see Fig. 1). The coordinates can be related to an arbitrary origin O and the z-axis is directed along the internuclear axis AB. The nuclear coordinates are $\vec{R}_\mathrm{A}$ and $\vec{R}_\mathrm{B}$ and the electrons coordinates are r_i with $i = 1, 2, \ldots$. The following geometrical relations exist for any of the electrons

$$\vec{R} = \vec{R}_\mathrm{B} - \vec{R}_\mathrm{A}; \quad \vec{r}_\mathrm{iA} = \vec{r}_i - \vec{R}_\mathrm{A}; \quad \vec{r}_\mathrm{iB} = \vec{r}_i - \vec{R}_\mathrm{B}$$

$$\vec{r}_\mathrm{iA} - \vec{r}_\mathrm{iB} = \vec{R}_\mathrm{B} - \vec{R}_\mathrm{A} = \vec{R}. \qquad (14)$$

In the central-field approximation the atomic orbitals from centers A and B are Dirac spinors in Eq. (2) which can be written in the form

$$\psi_a(\vec{r}) = \frac{f_a(|\vec{r}|)}{|\vec{r}|} \chi_{\ell_a, j_a \mu_a}(\vec{r}), \qquad \psi_b(\vec{r}) = \frac{f_b(|\vec{r}|)}{|\vec{r}|} \chi_{\ell_b, j_b \mu_b}(\vec{r}), \qquad (15)$$

where $f(r)$ describes the large P or small Q component of the radial one-electron wave function. The spin-orbit wave function $\chi_{\ell,j,\mu} = \chi_{\kappa\mu}$ in terms of the spherical harmonics $Y_{\ell,m}(\vec{r})$ is

$$\chi_{\ell,j,\mu}(\vec{r}) = \sum_{m,\sigma=\pm\frac{1}{2}} C_{\ell m, \frac{1}{2}\sigma}^{j\mu} Y_{\ell,m}(\vec{r}) \cdot \Phi_\sigma, \qquad (16)$$

where $\mathrm{C}_{\ell m, \frac{1}{2}\sigma}^{j\mu}$ are Clebsch-Gordan coefficients and Φ_σ is a spin function.

To accelerate convergence of the reexpansion we modified the standard Löwdin reexpansion procedure by dividing the range of integration into two exclusive regions V_A and V_B where we assume that the region V_A contains atom A and the region V_B contains atom B. We only apply the reexpansion procedure to the "tails" of wave functions occurring in a given region. To describe this we introduce the step-wise functions:

$$\Theta_A(\vec{r}) = \begin{cases} 1 & \vec{r} \in V_A \\ 0 & \vec{r} \in V_B \end{cases} \quad \text{and} \quad \Theta_\mathrm{B}(\vec{r}) = \begin{cases} 0 & \vec{r} \in V_A \\ 1 & \vec{r} \in V_B \end{cases} \qquad (17)$$

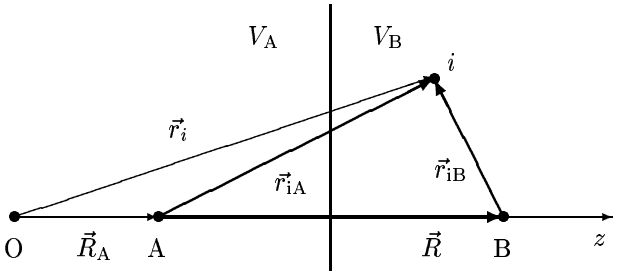

FIG. 1. Definition of nuclear and electron coordinates. The nuclei are located at A and B and the electron is located at i. The integration regions V_A and V_B are also shown.

The reexpansion of a wave function centered at B onto center A has the form

$$\Theta_A(\vec{r}) \cdot \frac{f_b(|\vec{r}_B|)}{|\vec{r}_B|} \chi_{\ell_b, j_b \mu_b}(\vec{r}_B) = \frac{1}{r_A} \sum_{\ell,j} \zeta_b(A, \ell, j, \mu_b | r_A) \times \chi_{\ell j \mu_b}(\vec{r_A}), \quad (18)$$

where

$$\begin{aligned} &\zeta_b(A, \ell, j, \mu_b | r_A) = \zeta_b(A, \kappa_b, \mu_b | r_A) \\ &= \sum_{m,\sigma} C_{\ell_b m \frac{1}{2}\sigma}^{j_b \mu_b} \cdot C_{\ell m, \frac{1}{2}\sigma}^{j \mu_b} \frac{K_{\ell m} K_{\ell_b m}}{R} \\ &\int_{\max(|r_A|, |R - r_A|)}^{|R + r_A|} dr_B f_b(r_B) \\ &\times P_{\ell_b}^{|m|}(|\frac{r_B^2 + R^2 - r_A^2}{2 r_B R}|) P_\ell^{|m|}(|\frac{r_A^2 + R^2 - r_B^2}{2 r_B R}|), \end{aligned} \qquad (19)$$

where $P_\ell^{|m|}$ are the standard associated Legendre polynomials, $\sigma = m$-μ and

$$K_{\ell m} = \sqrt{\frac{(2\ell + 1)}{2} \frac{(\ell - |m|)!}{(\ell + |m|)!}}.$$

Using symmetrical reexpansion the product of two wave functions, calculated on the different centers can be described as

$$\frac{f_a(r_A)}{r_A} \chi_{\ell_a, j_a \mu_a}(\vec{r}_A) \cdot \frac{f_b(r_B)}{r_B} \chi_{\ell_b, j_b \mu_b}(\vec{r}_B) = \qquad (20)$$

$$\frac{f_a(r_A)}{r_A}\chi_{\ell_a,j_a\mu_a}(\vec{r}_A)\frac{1}{r_A}\sum_{\ell,j}\zeta_b(A,\ell,j,\mu_a|r_A)\chi_{\ell,j\mu_b}(\vec{r}_A)$$
$$+\frac{f_b(r_B)}{r_B}\chi_{\ell_b,j_b\mu_b}(\vec{r}_B)\frac{1}{r_B}\sum_{\ell,j}\zeta_a(B,\ell,j,\mu_b|r_B)\chi_{\ell,j\mu_a}(\vec{r}_B).$$

Expression (20) is used to calculate the one- and two-electron two-center integrals. As an example we present the final expression for the overlap integral between orbitals α_i and β_j from $\det_\alpha^{AB}$ and $\det_\beta^{AB}$, respectively,

$$S_{i,j}^{\alpha\beta} = \int_0^\infty dr\Big\{P_a(r)\cdot\zeta_{P_b}(A,\kappa_a,\mu_a|r_A) + P_b(r)\cdot\zeta_{P_a}(B,\kappa_b,\mu_b|r_B)\Big\} + \int_0^\infty dr\Big\{Q_a(r)\cdot\zeta_{Q_b}(A,-\kappa_a,\mu_a|r_A) + Q_b(r)\cdot\zeta_{Q_a}(B,-\kappa_b,\mu_b|r_B)\Big\}. \quad (21)$$

V. COULOMB TYPE TWO-CENTER INTEGRALS

In this section we will find expressions for the Coulomb integrals, in a form convenient for computation, using the reexpanded atomic orbitals. We have extended the notation for the electron coordinates in the following way:

$$\vec{r}_{12} = \vec{r}_1 - \vec{r}_2$$

where the r_i and R_α are defined with respect to an arbitrary origin.

Following Eq. (13) the matrix elements for the Coulomb interaction are

$$\gamma_{ac,bd} = \int d\vec{r}_1 \int d\vec{r}_2 \frac{\rho_{a,c}(\vec{r}_{1A})\rho_{b,d}(\vec{r}_{2B})}{|\vec{r}_1-\vec{r}_2|}, \quad (22)$$

where $\rho_{a,c}(\vec{r}_{1A}) = \psi_a^*(\vec{r}_{1A})\cdot\psi_c(\vec{r}_{1A})$ and $\rho_{b,d}(\vec{r}_{2B}) = \psi_b^*(\vec{r}_{2B})\cdot\psi_d(\vec{r}_{2B})$ are densities of four-component electronic wave functions centered at A and B, respectively. Since the Coulomb potential for an electron density ρ is defined as

$$U(\vec{r}) = \int d\vec{r'}\frac{\rho(\vec{r'})}{|\vec{r}-\vec{r'}|}, \quad (23)$$

the Coulomb matrix elements Eq.(22) can be written as

$$\gamma_{ac,bd} = \int d\vec{r}_2\, U_{ac}(\vec{r}_{2\mathrm{A}})\rho_{bd}(\vec{r}_{2\mathrm{B}}). \quad (24)$$

Now we expand the densities $\rho(\vec{r})$ and Coulomb potentials $U(\vec{r})$ that are created by these densities in terms of the spherical harmonics. For $\rho_{a,c}(\vec{r})$ we have

$$\rho_{ac}(\vec{r}) = \sum_{\ell,m}\sqrt{\frac{(\ell+1)}{4\pi}}\cdot g^\ell(j_a\mu_a,j_c,\mu_c) \times Y_{\ell,m}(\vec{r})\cdot\rho_{ac}(r), \quad (25)$$

where $g^\ell(j\mu,j',\mu')$ are relativistic Gaunt coefficients:

$$g^\ell(j\mu,j',\mu') = \frac{\sqrt{(2j+1)(2j'+1)}}{2\ell+1}(-1)^{\mu'+\frac{1}{2}} \quad (26)$$
$$nonumber \quad (27)$$
$$\times C^{\ell,\mu-\mu'}_{j\mu,j'-\mu'}\ cdotC^{\ell,0}_{j-\frac{1}{2},j'\frac{1}{2}}, \quad (28)$$

and $\rho_{ac}(r)$ is the radial electronic density:

$$\rho_{ac}(r) = P_a(r)\cdot P_c(r) + Q_a(r)\cdot Q_c(r). \quad (29)$$

A similar expansion can be written for the density ρ_{bd} near center B. The potential $U_{ac}(\vec{r})$ can be introduced as

$$U_{ac}(\vec{r}) = \frac{1}{r}\sum_{k=|j_a-j_c|,\mu}^{j_a+j_c} v_{ac}^k(r)\cdot Y_{k,\mu}(\vec{r}), \quad (30)$$

where

$$v_{ac}^k(r) = \sqrt{\frac{4\pi}{2k+1}}g^k(j_a\mu_a,j_c\mu_c)\cdot\int dr'\rho_{ac}^k(r')\frac{(r_<)^k}{(r_>)^{k+1}} \quad (31)$$

A similar expression can be obtained for U_{bd}.

The integration region of $\vec{r}$ in Eq. (22) is divided in two half planes V_A and V_B and a surface S between the planes. Furthermore using the Laplace equation $\Delta U(\vec{r})=-4\pi\rho(\vec{r})$ and applying Green's theorem, we rewrite Eq. (24) as

$$\gamma_{ac,bd} = \gamma_{ac,bd}^{(V_A)} + \gamma_{ac,bd}^{(V_B)} + \gamma_{ac,bd}^{(S)}, \quad (32)$$

where

$$\gamma_{ac,bd}^{(V_A)} = \int_{V_A} d\vec{r}\,U_{ac}(\vec{r}_A)\rho_{bd}(\vec{r}_B),$$
$$\gamma_{ac,bd}^{(V_B)} = \int_{V_B} d\vec{r}\,U_{bd}(\vec{r}_B)\rho_{ac}(\vec{r}_A), \quad (33)$$
$$\gamma_{ac,bd}^{(S)} = -\frac{1}{4\pi}\int_S dS\ \Big[U_{ac}(\vec{r}_A)\frac{\partial}{\partial z}U_{bd}(\vec{r}_B) - U_{bd}(\vec{r}_B)\frac{\partial}{\partial z}U_{ac}(\vec{r}_A)\Big].$$

Using Eq. (30) and the symmetrical reexpansion of Eq. (18) for the density $\rho_{bd}(\vec{r}_B)$ around center A and for the density $\rho_{ac}(\vec{r}_A)$ around center B we obtain for the volume integrals

$$\gamma^{(V_A)}_{ac,bd} = \sum_{k}^{\ell_a+\ell_c}\sum_{k'}^{\ell_b+\ell_d} \int dr v^k_{ac}(r)\zeta_{bd}(A,k',\mu_d-\mu_b|r_A),$$
$$\gamma^{(V_B)}_{ac,bd} = \sum_{k}^{\ell_b+\ell_d}\sum_{k'}^{\ell_a+\ell_c} \int dr v^k_{bd}(r)\zeta_{ac}(B,k',\mu_a-\mu_c|r_B) \quad (34)$$

For the surface (S) integrals we have

$$\gamma^{(S)}_{ac,bd} = \sum_{k}^{\ell_a+\ell_c}\sum_{k'}^{\ell_b+\ell_d} \left(\frac{1}{R}v^k_{ac}(\frac{R}{2})v^{k'}_{bd}(\frac{R}{2})\cdot\delta_{\mu,0} - 4\pi\int_{R/2}^{\infty} dr\frac{1}{r}v^k_{ac}(\frac{R}{2})v^{k'}_{bd}(\frac{R}{2}) \times \frac{\partial[Y_{k,\mu}(R/2r,0)\cdot Y^*_{k',\mu}(R/2r,0)]}{\partial R}\right), \quad (35)$$

where $\mu=\mu_a-\mu_c=\mu_d-\mu_b$.

VI. EXCHANGE TYPE INTEGRALS

The exchange type interaction matrix element is

$$h_{ac,bd} = \int d\vec{r}_1\int d\vec{r}_2\cdot\psi^*_a(\vec{r}_{1A})\cdot\psi_b(\vec{r}_{1B})\frac{1}{r_{12}} \times\psi_c(\vec{r}_{2A})\cdot\psi^*_d(\vec{r}_{2B}) \quad (36)$$

where $\psi(\vec{r})$ is defined by Eq.(2), a,c denote one-electron functions centered at A, and b,d denote functions centered at B.

We can separate the relativistic exchange type integral into a part for the large component P and a part for the small component Q:

$$h_{ac,bd} = h^P_{ac,bd} + h^Q_{ac,bd} \quad (37)$$

Let us consider the integral $h^P_{ac,bd}$ for the large component. Equivalent expressions for the small component integrals can be derived. For the product of functions of different centers we use the two-center expansion formula (20). The spatial integrations for the exchange type integral is divided in four parts via

$$\int d\vec{r}_1\int d\vec{r}_2 = \left(\int_{V_A} d\vec{r}_1+\int_{V_B} d\vec{r}_1\right) \times\left(\int_{V_A} d\vec{r}_2+\int_{V_B} d\vec{r}_2\right),$$

where the half planes $V_{\rm A,B}$ are defined in Fig. 1. Hence the exchange type integral has the four contributions

$$h^P_{ac,bd} = h^{P,(AA)}_{ac,bd} + h^{P,(BB)}_{ac,bd} + h^{P,(AB)}_{ac,bd} + h^{P,(BA)}_{ac,bd}, \quad (38)$$

where the first two terms of Eq. (38) correspond to integrals where the wave functions of electrons 1 and 2 are in overlapping region and the last two terms of Eq. (38) are related to integrals where the wave functions are in non-overlapping region. Using an expansion of the Coulomb interaction $1/r_{12}$ around center A in terms of spherical harmonics

$$\frac{1}{r_{12}} = 4\pi\sum_{k=0}^{\infty}\frac{1}{2k+1}u_k(r_{1A},r_{2A})\sum_{\mu}Y_{k\mu}(\vec{r}_{1A})Y^*_{k\mu}(\vec{r}_{2A}),$$

where $u_k(r_1,r_2)=r^k_</r^{k+1}_>$, we have for terms with overlapping wave functions

$$h^{P,(AA)}_{ac,bd} = \sum_{jl}\sum_{j'l'}\sum_{k} g^k(j_a\mu_a,j\mu_c)\cdot g^k(j_d\mu_d,j'\mu_b) \times\int_0^{\infty} dr_2 P_d(r_2)\ \zeta_b(A,l',j',\mu_b|r_2) \times\int_0^{\infty} dr_1 P_a(r_1)\ \zeta_c(A,l,j,\mu_c|r_1)\ u_k(r_1,r_2)\,. \quad (39)$$

The integral $h^{P,(BB)}_{ac,bd}$ is solved similarly. The integrals $h^{P,(AB)}_{ac,bd}$ and $h^{P,(BA)}_{ac,bd}$ are evaluated using techniques similar to those in Section V.

The main complexity in evaluating exchange type integrals is that it includes infinite sums. These expansions however converge very fast due to the symmetrical reexpansion procedure. It is sufficient to use 8 to 10 terms in expansion (39) to obtain exchange type integrals with an accuracy of 10^{-6}.

VII. METASTABLE XE_2

We now use the RCIVB method, described in above sections, to calculate the electronic potentials of metastable Xe_2. Xe atom has 54 electrons and in the calculation we define the 48 electrons in the closed shells $1s^22s^22p^6...5s^2$ of each Xe atom as the core. An R-dependent all-electron core potential is calculated exactly and included in the Hamiltonian. The outer $5p^5$ and $6s$ orbitals of metastable Xe are valence orbitals. Furthermore we use the Sturmian $6p, 5d, 7s$ virtual or unoccupied orbitals to enhance the correlation. Various covalent and ionic configurations are constructed by distributing electrons from the $5p^56s$ configuration over the relativistic $5p^2_{1/2}$, $5p^3_{3/2}$, $6s_{1/2}$, $6p_{1/2}$, $6p_{3/2}$, $5d_{3/2}$, $5d_{5/2}$, and $7s_{1/2}$ orbitals. In total there are 97 relativistic configurations in our CI expansion. This particular choice of configurations which ignores the $5p^1_{1/2}5p^4_{3/2}$nl configurations, takes into account the majority of the correlation and restricts the number of one and two electron integrals to a manageable number. In total we construct 1991 molecular determinants from these configurations. The list of configurations is given in Table I. For clarity the molecular configurations with atomic configurations interchanged are not listed in Table I but they are included in our calculation. This ensures that the gerade ("g")/ungerade ("u") symmetry of molecule is satisfied.

The configurations are divided into several groups on the basis of their role in the formation of the molecule. The first line in the table describes the core orbitals. The metastable Xe $5p^5 6s + 5p^5 6s$ is the leading valence configuration.

The next group of configurations include configurations where one Xe atom is in the metastable state and the other Xe atom is in a higher excited state that has the same parity as the metastable atom. These configurations serve to obtain a correct description of the metastable atom and consequently a correct dissociation limit for the molecule. The group of configurations with "opposite parity" include two atomic configurations of opposite parity and contribute to the formation of a molecule at short and intermediate internuclear separation.

Two groups of configurations contribute to the long-range polarization interactions between metastable atoms. These are the "C_6" and "C_8" configurations, which give rise to the induced dipole-dipole $-C_6/R^6$ and to the induced dipole-quadrapole $-C_8/R^8$ interactions, respectively. The next group are the so called "ionic" configurations, where participating atoms have positive and negative charges. These configurations contribute at short internuclear separation. The last group of configurations presents so called "other neutral" configurations and include configurations which do not play a significant role in the molecular formation. Some of these configurations contribute to the atomic structure.

The use of physically realistic configurations in the CI ensures that molecular quantities such as dissociation energies, exchange and Coulomb type interactions and dipole-dipole long-range interactions are introduced correctly. Later we demonstrate our ability to analyze the influence of each group of configurations on the formation of the molecule by plotting the configuration weights as function of internuclear separation. The configuration weights are sensitive indicators of the molecular wave function.

The configuration weights for each state of the seven groups are determined by diagonalizing the matrix H_{AB}. Since there are many eigenstates which have a lower energy than the metastable potentials we applied direct diagonalization instead of a Davidson iterative procedure.

For the present calculation we focus on the lowest metastable potentials of Xe_2 which are accessible in experiments with ultra-cold metastable Xe [28]. These potentials dissociate to the three limits $(5p^5 6s + 5p^5 6s)$ $[3/2]_2 + [3/2]_2$, $[3/2]_2 + [3/2]_1$ and $[3/2]_1 + [3/2]_1$ and have a projection of their total electron angular momentum along the internuclear axis $\Omega = 0, 1, 2, 3, 4$. The atomic notation is explained in Ref. [29]. The metastable potentials are identified from a comparison with experimental atomic energies [29], the degeneracy at the dissociation limit for a given Ω and the CI weights.

TABLE I. Molecular configurations used in the calculations.

Atom A		Atom B	Description
$1s^2_{1/2}...5s^2_{1/2}$	+	$1s^2_{1/2}...5s^2_{1/2}$	core
$5p^2_{1/2}5p^3_{3/2}6s_{1/2}$	+	$5p^2_{1/2}5p^3_{3/2}6s_{1/2}$	metastable
$5p^2_{1/2}5p^3_{3/2}6s_{1/2}$	+	$5p^2_{1/2}5p^3_{3/2}5d_{5/2}$	same parity
$5p^2_{1/2}5p^3_{3/2}6s_{1/2}$	+	$5p^2_{1/2}5p^3_{3/2}5d_{3/2}$	
$5p^2_{1/2}5p^3_{3/2}6s_{1/2}$	+	$5p^2_{1/2}5p^3_{3/2}7s_{1/2}$	
$5p^2_{1/2}5p^3_{3/2}5d_{3/2}$	+	$5p^2_{1/2}5p^3_{3/2}5d_{3/2}$	
$5p^2_{1/2}5p^3_{3/2}5d_{5/2}$	+	$5p^2_{1/2}5p^3_{3/2}5d_{5/2}$	other neutral
$5p^2_{1/2}5p^3_{3/2}5d_{3/2}$	+	$5p^2_{1/2}5p^3_{3/2}5d_{5/2}$	
$5p^2_{1/2}5p^3_{3/2}5d_{3/2}$	+	$5p^2_{1/2}5p^3_{3/2}7s_{1/2}$	
$5p^2_{1/2}5p^3_{3/2}5d_{5/2}$	+	$5p^2_{1/2}5p^3_{3/2}7s_{1/2}$	
$5p^2_{1/2}5p^3_{3/2}7s_{1/2}$	+	$5p^2_{1/2}5p^3_{3/2}7s_{1/2}$	
$5p^2_{1/2}5p^2_{3/2}6s^2_{1/2}$	+	$5p^2_{1/2}5p^4_{3/2}$	
$5p^2_{1/2}5p^3_{3/2}6s_{1/2}$	+	$5p^2_{1/2}5p^4_{3/2}$	
$5p^2_{1/2}5p^3_{3/2}5d_{3/2}$	+	$5p^2_{1/2}5p^4_{3/2}$	
$5p^2_{1/2}5p^3_{3/2}5d_{5/2}$	+	$5p^2_{1/2}5p^4_{3/2}$	
$5p^2_{1/2}5p^3_{3/2}6p_{1/2}$	+	$5p^2_{1/2}5p^4_{3/2}$	
$5p^2_{1/2}5p^3_{3/2}6p_{3/2}$	+	$5p^2_{1/2}5p^4_{3/2}$	
$5p^2_{1/2}5p^3_{3/2}7s_{1/2}$	+	$5p^2_{1/2}5p^4_{3/2}$	
$5p^2_{1/2}5p^4_{3/2}$	+	$5p^2_{1/2}5p^4_{3/2}$	
$5p^2_{1/2}5p^3_{3/2}6p_{1/2}$	+	$5p^2_{1/2}5p^3_{3/2}7s_{1/2}$	
$5p^2_{1/2}5p^3_{3/2}6p_{3/2}$	+	$5p^2_{1/2}5p^3_{3/2}7s_{1/2}$	
$5p^2_{1/2}5p^3_{3/2}6s_{1/2}$	+	$5p^2_{1/2}5p^3_{3/2}6p_{1/2}$	opposite parity
$5p^2_{1/2}5p^3_{3/2}6s_{1/2}$	+	$5p^2_{1/2}5p^3_{3/2}6p_{3/2}$	
$5p^2_{1/2}5p^3_{3/2}6p_{1/2}$	+	$5p^2_{1/2}5p^3_{3/2}6p_{1/2}$	C_6
$5p^2_{1/2}5p^3_{3/2}6p_{3/2}$	+	$5p^2_{1/2}5p^3_{3/2}6p_{3/2}$	
$5p^2_{1/2}5p^3_{3/2}6p_{1/2}$	+	$5p^2_{1/2}5p^3_{3/2}6p_{3/2}$	
$5p^2_{1/2}5p^3_{3/2}5d_{3/2}$	+	$5p^2_{1/2}5p^3_{3/2}6p_{3/2}$	C_8
$5p^2_{1/2}5p^3_{3/2}5d_{3/2}$	+	$5p^2_{1/2}5p^3_{3/2}6p_{1/2}$	
$5p^2_{1/2}5p^3_{3/2}5d_{5/2}$	+	$5p^2_{1/2}5p^3_{3/2}6p_{1/2}$	
$5p^2_{1/2}5p^3_{3/2}5d_{5/2}$	+	$5p^2_{1/2}5p^3_{3/2}6p_{3/2}$	
$5p^2_{1/2}5p^3_{3/2}$	+	$5p^2_{1/2}5p^3_{3/2}6s_{1/2}5d_{3/2}$	ionic
$5p^2_{1/2}5p^3_{3/2}$	+	$5p^2_{1/2}5p^3_{3/2}5d_{3/2}5d_{5/2}$	
$5p^2_{1/2}5p^3_{3/2}$	+	$5p^2_{1/2}5p^3_{3/2}6s_{1/2}5d_{5/2}$	
$5p^2_{1/2}5p^3_{3/2}$	+	$5p^2_{1/2}5p^3_{3/2}6s_{1/2}6p_{1/2}$	
$5p^2_{1/2}5p^3_{3/2}$	+	$5p^2_{1/2}5p^3_{3/2}5d_{3/2}6p_{1/2}$	
$5p^2_{1/2}5p^3_{3/2}$	+	$5p^2_{1/2}5p^3_{3/2}5d_{5/2}6p_{3/2}$	
$5p^2_{1/2}5p^3_{3/2}$	+	$5p^2_{1/2}5p^3_{3/2}6s_{1/2}6p_{3/2}$	
$5p^2_{1/2}5p^3_{3/2}$	+	$5p^2_{1/2}5p^3_{3/2}6p_{1/2}6p_{3/2}$	
$5p^2_{1/2}5p^3_{3/2}$	+	$5p^2_{1/2}5p^3_{3/2}5d_{5/2}6p_{1/2}$	
$5p^2_{1/2}5p^3_{3/2}$	+	$5p^2_{1/2}5p^3_{3/2}5d_{3/2}6p_{3/2}$	
$5p^2_{1/2}5p^3_{3/2}$	+	$5p^2_{1/2}5p^3_{3/2}6s^2_{1/2}$	
$5p^2_{1/2}5p^3_{3/2}$	+	$5p^2_{1/2}5p^3_{3/2}5d^2_{3/2}$	
$5p^2_{1/2}5p^3_{3/2}$	+	$5p^2_{1/2}5p^3_{3/2}5d^2_{5/2}$	
$5p^2_{1/2}5p^3_{3/2}$	+	$5p^2_{1/2}5p^3_{3/2}6p^2_{1/2}$	
$5p^2_{1/2}5p^3_{3/2}$	+	$5p^2_{1/2}5p^3_{3/2}6p^2_{3/2}$	
$5p^2_{1/2}5p^3_{3/2}$	+	$5p^2_{1/2}5p^3_{3/2}7s^2_{1/2}$	
$5p^2_{1/2}5p^3_{3/2}$	+	$5p^2_{1/2}5p^3_{3/2}6s_{1/2}7s_{1/2}$	
$5p^2_{1/2}5p^3_{3/2}$	+	$5p^2_{1/2}5p^4_{3/2}6p_{1/2}$	
$5p^2_{1/2}5p^3_{3/2}$	+	$5p^2_{1/2}5p^4_{3/2}6s_{1/2}$	
$5p^2_{1/2}5p^3_{3/2}$	+	$5p^2_{1/2}5p^4_{3/2}7s_{1/2}$	
$5p^2_{1/2}5p^3_{3/2}$	+	$5p^2_{1/2}5p^4_{3/2}5d_{3/2}$	
$5p^2_{1/2}5p^3_{3/2}$	+	$5p^2_{1/2}5p^4_{3/2}6p_{3/2}$	
$5p^2_{1/2}5p^3_{3/2}$	+	$5p^2_{1/2}5p^4_{3/2}5d_{5/2}$	

The potentials are used to obtain molecular constants of metastable Xe_2. The equilibrium distance, R_e, rotational, ω_e, and vibrational, B_e, frequencies at R_e, and the dissociation energy, D_e, are shown in Table II. Potentials in Table II are ordered with increasing total energy. The second column numbers the potentials. The first column of Table II indicates the symmetry labels of the potentials. In relativistic notation these correspond to the projection quantum number Ω and "g" and "u" symmetry. Table III describes the molecular dissociation limits of the potentials shown in Table II.

As an example of the structure of the metastable potentials, we show in Fig. 2 the potentials with Ω=0, that dissociate to the lowest metastable atomic $5p^5 6s$ levels. The potentials create three groups of curves with R_e between 10 a.u. and 13.3 a.u., 12.5 a.u. and 14.1 a.u., and 12.4 a.u. and 13.7 a.u.. The curves do not exhibit strong avoided crossings. For $\Omega = 0$ there are eight "g" potentials and six "u" potentials. The splittings between the three dissociation limits are related to the $J = 1$ and $J = 2$ fine-structure splitting of the $5p^5 6s$ [3/2] term. These splittings are in a good agreement (7%) with experimental atomic data [29] where the experimental difference between the two metastable atomic levels $[3/2]_2$ and $[3/2]_1$ is $\Delta E_{exp.} = 977.6$ cm^{-1} which is compared to the energy distance between the two lowest molecular dissociation limits in Fig. 2. The energy difference between the first and the third limit in Fig. 2 agrees to the same level of accuracy with twice the atomic energy difference $\Delta E_{exp.}$.

TABLE II. Molecular constants of $\mathbf{Xe}_2$ potentials dissociating to $(5p^5 6s + 5p^5 6s)$ states. (The energy equivalent 1 cm^{-1} is 29.9792458 GHz.)

$\Omega_{g/u}$	Index	R_e (a.u.)	ω_e (cm^{-1})	B_e (cm^{-1})	D_e (cm^{-1})
0_g	1	10.0	18.3	0.0046	1650
0_u	2	10.0	19.0	0.0046	1636
0_u	3	10.4	23.4	0.0043	1533
0_g	4	10.4	24.0	0.0042	1517
0_g	5	13.3	7.6	0.0026	314
0_u	6	12.5	12.8	0.0029	856
0_g	7	12.6	11.0	0.0029	579
0_u	8	13.2	8.6	0.0026	366
0_g	9	13.5	7.3	0.0025	296
0_u	10	13.5	7.3	0.0025	295
0_g	11	14.1	6.7	0.0023	239
0_g	12	12.4	6.6	0.0030	649
0_u	13	12.6	6.7	0.0029	566
0_g	14	13.7	10.7	0.0024	348
1_u	1	10.4	18.8	0.0042	1606
1_g	2	10.2	20.6	0.0044	1576
1_u	3	10.3	22.0	0.0042	1525
1_g	4	13.3	7.1	0.0026	306
1_u	5	12.5	12.8	0.0029	855
1_g	6	12.6	11.2	0.0029	581
1_u	7	13.1	8.8	0.0027	365
1_g	8	13.6	6.7	0.0025	278
1_u	9	13.6	7.5	0.0025	278
1_g	10	14.1	6.6	0.0023	235
1_u	11	13.0	10.5	0.0027	514
1_g	12	13.4	7.1	0.0026	381
2_g	1	10.2	20.4	0.0044	1596
2_u	2	10.2	20.6	0.0044	1515
2_g	3	13.4	7.2	0.0025	284
2_u	4	12.4	13.0	0.0030	851
2_g	5	12.6	11.6	0.0029	585
2_g	6	13.7	6.7	0.0024	254
2_u	7	14.0	6.5	0.0023	227
2_g	8	13.1	7.0	0.0027	412
3_u	1	9.93	20.41	0.0046	1521
3_g	2	13.5	6.85	0.0025	255
3_u	3	12.3	13.44	0.0030	844
3_g	4	13.6	6.81	0.0025	258
4_g	1	13.6	6.43	0.0025	228

TABLE III. Dissociation limits of $\mathbf{Xe}_2$ potentials from Table II.

Ω	Indices from Table II	Dissociation limit
0	1 - 5	$[3/2]_2 + [3/2]_2$
	6 - 11	$[3/2]_2 + [3/2]_1$
	12 - 14	$[3/2]_1 + [3/2]_1$
1	1 - 4	$[3/2]_2 + [3/2]_2$
	5 - 10	$[3/2]_2 + [3/2]_1$
	11, 12	$[3/2]_1 + [3/2]_1$
2	1-3	$[3/2]_2 + [3/2]_2$
	4-7	$[3/2]_2 + [3/2]_1$
	8	$[3/2]_1 + [3/2]_1$
3	1,2	$[3/2]_2 + [3/2]_2$
	3,4	$[3/2]_2 + [3/2]_1$
4	1	$[3/2]_2 + [3/2]_2$

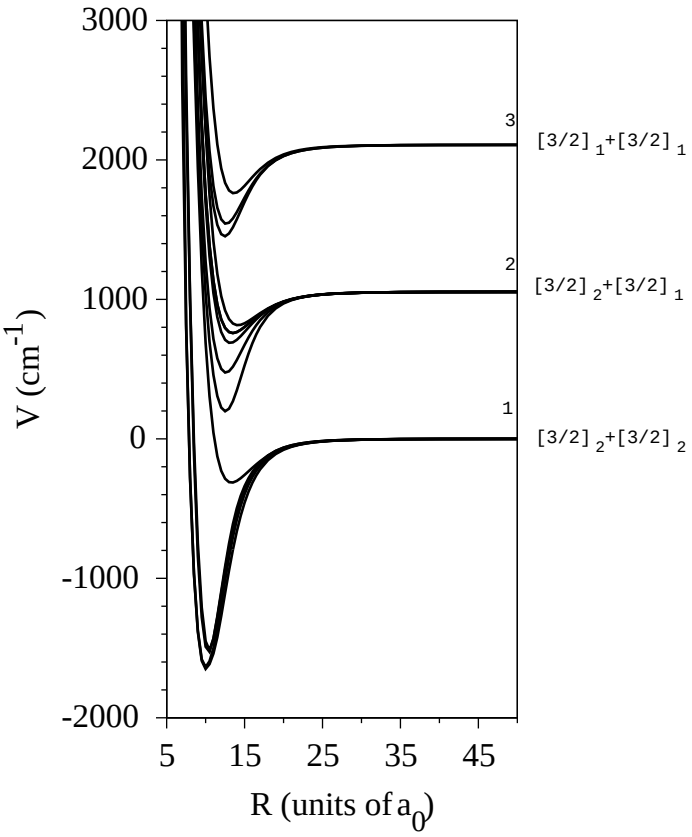

FIG. 2. The $\Omega = 0$ metastable $5p^5 6s + 5p^5 6s$ Xe potentials as a function of internuclear separation.

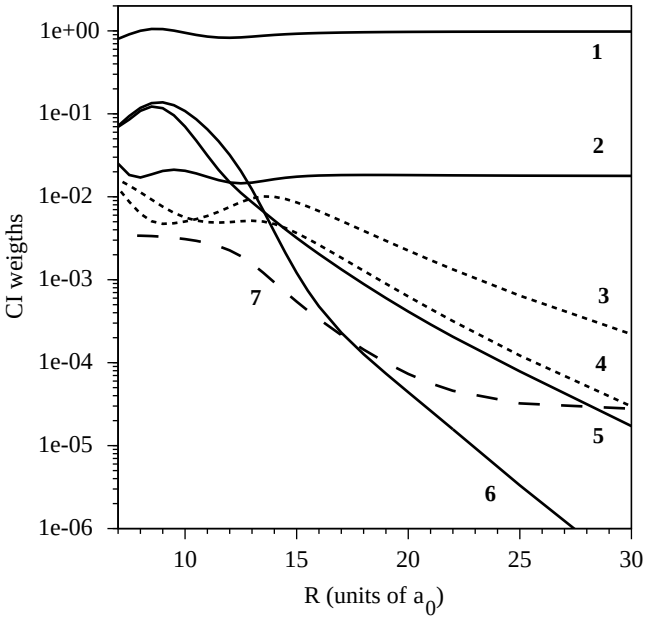

FIG. 3. The configuration interaction weights of the lowest level of Ω=3 as a function of internuclear separation. The six lines correspond with 1) the metastable configuration, 2) configurations with the same parity as a metastable, 3) "C_6" configurations, 4) "C_8" configurations", 5) "ionic" configurations, 6) configurations with "opposite parity", 7) "other neutral" configurations.

Along with the potential energy surfaces we evaluated the CI weights of the potentials. These weights are the square of the CI amplitudes of Eq. (3). Figures 3 and 4 show the summed weights of the groups of configurations defined in Table I for the g and u lowest $\Omega = 3$ curves as function of internuclear separation. The weight of each group is obtained as the sum of all CI weights of determinants that belong to the configurations of this group. The two $\Omega = 3$ potentials are quantitatively different. From Table II we see that the lowest curve is much deeper and has an equilibrium distance at approximately 10 a.u. The second potential has an equilibrium distance of 13.5 a.u. For both figures the metastable configuration has the largest CI weight. Figs. 3 and 4 also show there exist two distinctive regions of internuclear separations where the curves are qualitatively different. For R$\leq$ 14 a.u. there is very "strong" configuration interaction. Many configurations contribute to the formation of the molecule. Except for the metastable configuration the CI weights of different groups have similar values.

This situation changes for larger internuclear separations. The CI weights have a more smooth and predictable behavior as function of R. For example, the "opposite" parity configurations show an exponential behavior consistent with the fact that these configurations can only contribute when the atomic wave function overlap. The "C_6" and "C_8" weights have a $1/R^6$ and $1/R^8$ behavior, respectively. Notice also the "other neutral" group includes configurations which contribute to the atomic structure, and the CI weight of this group has a finite value at large internuclear separations.

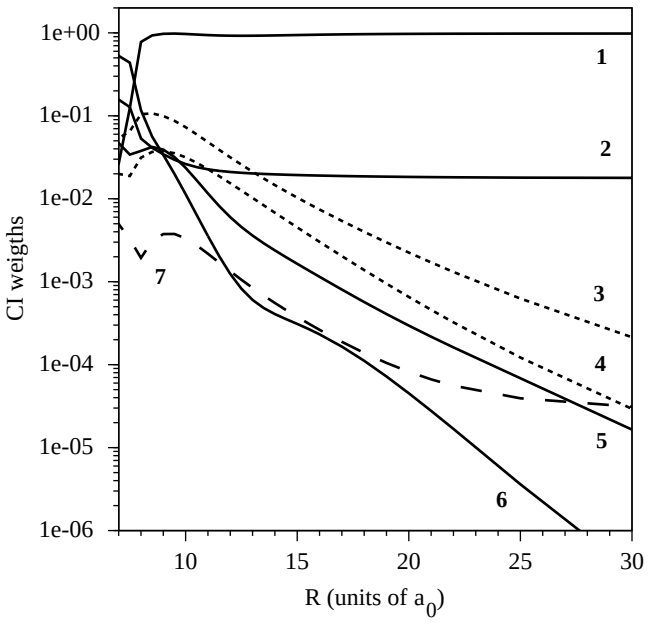

FIG. 4. The configuration interaction weights of the second level of Ω=3 as a function of internuclear separation. The lines have the same interpretation as those of Fig. 3

VIII. RELATIVISTIC EFFECTS

An important check on any relativistic theory is its convergence to a non-relativistic limit when the speed of light goes to infinity. In fact, the difference between the relativistic and the "c $\rightarrow \infty$" potentials shows the value of relativistic effects embedded in the Dirac equations including the spin-orbit interaction. The knowledge of these relativistic effects for core and valence electrons can be used in semi empirical and effective potential approaches to construct realistic potentials.

To provide this data we performed three calculations: relativistic, applying the RCIVB method, non-relativistic, using the relativistic code with the speed of light set to 10^4 x c, and a non-relativistic based on a CIVB method [22] using Hartree-Fock orbitals. We find that the total relativistic core energy is 430.06 a.u.(1 a.u.= 4.359743×10^{-18} J) lower than the total non-relativistic core energy. The valence energies are different as well. Fig. 5 presents the valence energies of the two lowest $\Omega = 3$ potentials, calculated in the three different approximations: relativistic, "c$\rightarrow \infty$", and non-relativistic as function of a internuclear separation. Comparing these results shows that when c $\rightarrow \infty$ the relativistic code converges to the non-relativistic limit (see the top four solid and dotted curves in Fig. 5). We explain the small difference between the two results by the fact that our CI expansion does not include configurations with $5p^1_{1/2}$ $5p^4_{3/2}$ shells in our calculation in order to avoid unacceptably large matrices. This means that we do not provide a complete set of relativistic configurations belonging to non-relativistic configurations with a $5p^5$ shell, which is the necessary condition for a complete convergence.

Moreover, comparison of relativistic and non-relativistic curves in Fig. 5 shows that the contraction of relativistic orbitals leads to a shorter equilibrium distance. For example, for the lowest potential R_e is smaller by 0.21 a.u.. For the same potential the non-relativistic dissociation energy is bigger by 230 cm^{-1}.

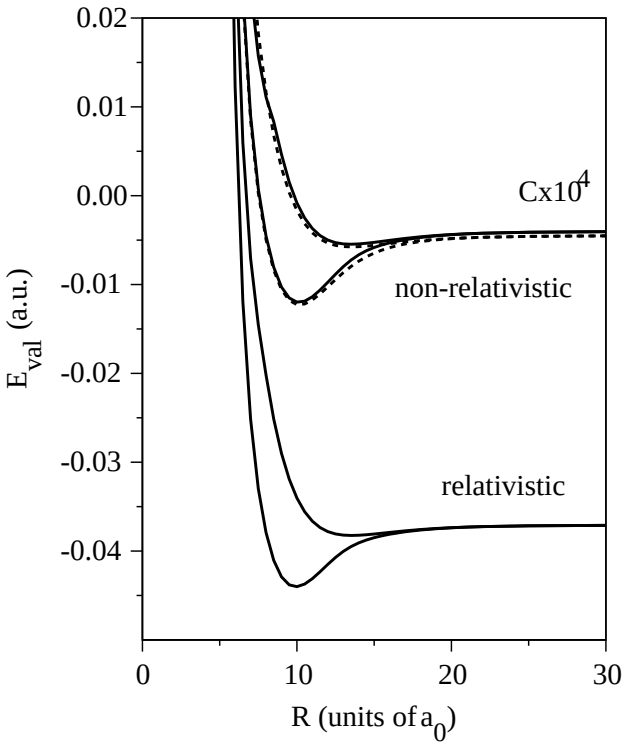

FIG. 5. The valence energy calculated in relativistic (bottom two solid lines), "c$\rightarrow \infty$"(upper two solid lines), and non-relativistic (dotted lines) approximations for the two lowest $\Omega = 3$ potentials of metastable Xe_2.

IX. CONCLUSIONS

We presented a new version of the *ab initio* relativistic configuration interaction valence bond method. The method uses nonorthogonal four-component Dirac-Fock orbitals and relativistic Sturmian wave functions. To further optimize these functions we introduced fractional occupation of the orbitals and density matrices of mixed states that correspond to the configuration average. The physically realistic atomic orbitals in our model lead to a compact description of a molecule and to an efficient configuration interaction procedure.

For a long time it has been thought that the use of numerical atomic wave functions in a molecular basis leads to a complex calculation of the many-center integrals. Here we develop a symmetric reexpansion procedure which ensures a fast convergence of the reexpansion.

We apply our method to a calculation of the electronic potentials of metastable Xe_2 dimer which is relevant for ultra-cold collisions. This application demonstrates the ability of the valence bond theory to provide a physically realistic description of interacting atoms.

We investigated the reliability of the model by comparing the electronic structure near the molecular dissociation limits with the corresponding energy structure of metastable Xe atom which is known experimentally. The structures are found to be in good agreement. The difference between relativistic and non-relativistic total energies of metastable Xe_2 is large and highlights the importance of a non-perturbative relativistic approach. Relativistic effects on the shape of the potentials show a contraction of bond lengths and a slight decreasing of the binding energies.

---

[1] R. McWeeny, *Methods of Molecular Quantum Mechanics* eds. D.P Craig., R. McWeeny, (Academic Press, London, 1992).

[2] D.J. Klein and N. Trinajstic, *Valence bond theory and chemical structures* (Elsevier, Amsterdam, 1990).

[3] W. Heitler and F. London, Z. Physik, **44**, 455 (1927).

[4] C. A. Coulson and I. H. Fischer, Phil. Mag., **40**, 386 (1949).

[5] W. A. Goddard, Phys. Rev. **157**, 73, 81 (1967).

[6] J. Gerratt and W. N. Lipscomb, Proc. natn. Acad. Sci. U.S.A. **59**, 332 (1968).

[7] J. Gerratt, Adv. atom. mol. Phys. **7**, 141 (1971).

[8] S. Wilson and J. Gerratt, Molec. Phys., **30**, 777 (1975).

[9] N.C. Pyper and J. Gerratt, Proc. R. Soc. Lond. A, **355**, (1977).

[10] D.L. Cooper, J. Gerratt, and M. Raimondi, Adv. Chem. Phys., **69**, 319 (1987).

[11] D.L. Cooper, J. Gerratt, and M. Raimondi, Int. Rev. Phys. Chem., **7**, 59 (1988).

[12] D.L. Cooper, J. Gerratt, and M. Raimondi, Top. Curr. Chem., **153**, 41 (1990); (*Advances in the Theory of Benzenoid Hydrocarbons*, I. Gutman, S. J. Cyvin, Eds.).

[13] D.L. Cooper, J. Gerratt, and M. Raimondi, Mol. Simulation, **4**, 293 (1990).

[14] D.L. Cooper, J. Gerratt, and M. Raimondi, Chem. Rev., **91**, 929 (1991).

[15] J. Gerratt, D.L. Cooper, P.B. Karadakov and M. Raimondi, Chem. Soc. Revs. **26**, 87 (1997).

[16] J. Langlois, R. Miller, T. Coley, W. Goddard III, M. Ringnalda, Y. Won, and R. Friesner, J. Chem. Phys. **92**, 7488 (1990).

[17] R. Miller, J. Langlois, M. Ringnalda, R. Friesner, and W. Goddard III, J. Chem. Phys. **100**, 1226 (1994).

[18] D. Tannor, B. Martin, R. Murphy, R. Friesner, D. Sitkoff, A. Nicholls, M. Ringnalda, W. Goddard III, and B. Honig, J. Am. Chem. Soc. **116**, 11875 (1994).

[19] S. Kotochigova and I. Tupitsyn, Int. J. Quant. Chem. **29**, 307 (1995).

[20] S. Kotochigova and I. Tupitsyn, J. Res. Natl. Inst. Stand. Technol., **103**, 201 (1998).

[21] S. Kotochigova and I. Tupitsyn, J. Res. Natl. Inst. Stand. Technol., **103**, 205 (1998).

[22] S. Kotochigova, E. Tiesinga, and I. Tupitsyn, Phys. Rev. A, in press (1999).

[23] J. C. Slater, *The self-consistent field for molecules and solids* vol. 4, N.Y., McGraw-Hill, (1974).

[24] P. P. Pavinsky and A. I. Sherstuk, *Problems of the theoretical physics*, Leningrad, vol. 1 (1974).

[25] A. I. Sherstuk, Opt. Spectrosc. **38**, 601 (1975).

[26] P.O. Löwdin, Advances in Physics, **5** 1 (1956).

[27] M. R. Doery, E. J. D. Vredenbregt, S. S. Op de Beek, H. C. W. Beijerinck, and B. J. Verhaar, Phys. Rev. A **58**, 3673 (1998).

[28] C. Orzel, S. D. Bergeson, S. Kulin, and S. L. Rolston, Phys. Rev. Lett. **80**, 5093 (1998).

[29] C. E. Moore, *Atomic Energy Levels*, NBS, Washington, D.C., 1952.